Article

Ferroelectric Liquid Crystals Induced by Dopants with Axially Chiral 2,2‘-Spirobiindan-1,1‘-dione Cores

Christopher J. Boulton, Jeremy G. Finden, Eagranie Yuh, Jeffrey J. Sutherland, Michael D. Wand, Gang Wu, and Robert P. Lemieux

J. Am. Chem. Soc., **2005**, 127 (39), 13656-13665• DOI: 10.1021/ja054322k • Publication Date (Web): 08 September 2005

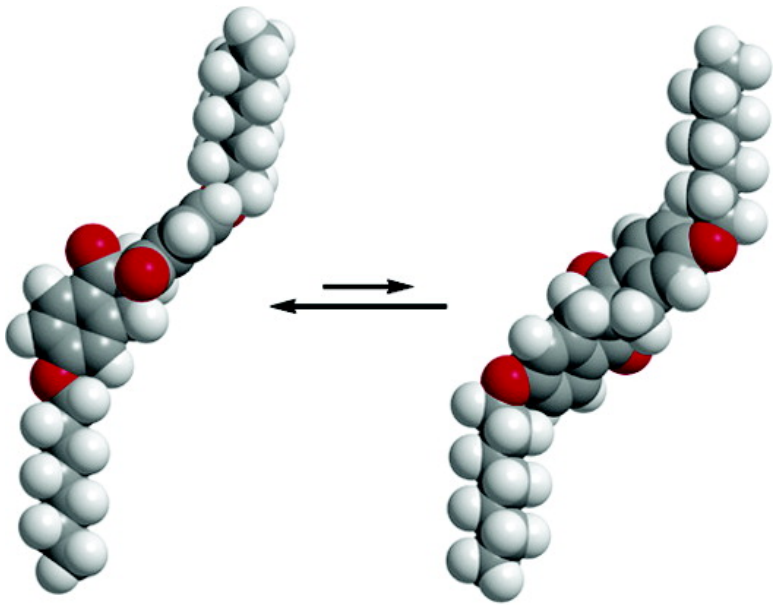

J|A|C|S
ARTICLES
Published on Web 09/08/2005

Ferroelectric Liquid Crystals Induced by Dopants with Axially Chiral 2,2′-Spirobiindan-1,1′-dione Cores

Christopher J. Boulton,[†] Jeremy G. Finden,[†] Eagranie Yuh,[†] Jeffrey J. Sutherland,[†] Michael D. Wand,[‡] Gang Wu,[†] and Robert P. Lemieux*,[†]

Contribution from the Department of Chemistry, Queen's University, Kingston, Ontario, Canada K7L 3N6, and Displaytech, Inc., 2602 Clover Basin Drive, Longmont, Colorado 80503

Received June 30, 2005; E-mail: lemieux@chem.queensu.ca

Abstract: The axially chiral dopants (*R*)-5,5′-, 5,6′-, and 6,6′-diheptyloxy-2,2′-spirobiindan-1,1′-dione ((*R*)-**2**, -**3**, and -**4**) were synthesized in optically pure form, and their absolute configurations were assigned by the exciton chirality method using circular dichroism spectroscopy. These new compounds were doped in four achiral liquid crystal hosts to give chiral smectic C* (SmC*) phases with spontaneous polarizations (P_S) that vary with the core structure of the host. The spontaneous polarization induced by the 5,5′-dialkoxy derivative (*R*)-**2** is uniformly positive, whereas that induced by the 6,6′-dialkoxy derivative (*R*)-**4** is uniformly negative and shows a different trend in host dependence. Polarization power (δ_p) values range from +21 nC/cm^2 for (*R*)-**2** in 2′,3′-difluoro-4-heptyl-4″-nonyl-*p*-terphenyl (**DFT**) to −1037 nC/cm^2 for (*R*)-**4** in 4-(4′-heptyl[1,1′-biphen]-4-yl)-1-hexylcyclohexanecarbonitrile (**NCB76**). The unsymmetrical dopant (*R*)-**3** behaves like a hybrid of the two symmetrical isomers, with lower absolute values of δ_p, on average, and varying signs of P_S. ^{2}H NMR spectra of the doped mixtures using racemic mixtures of **2**−**4** with $-OCD_2C_6H_{13}$ side-chains, in combination with phase diagrams, show that relatively minor changes in the dopant structure, that is, moving the alkoxy side-chains from the 5,5′ to the 6,6′ positions of the spirobiindandione core, have profound effects on dopant−host compatibility, and on the propensity of the dopant to exert chiral perturbations in the host environment. The variations in sign and magnitude of δ_p as a function of alkoxy group positions are rationalized based on an analysis of zigzag conformations that conform to the binding site of the SmC host according to the Boulder model.

Introduction

Liquid crystals are ordered fluids in which intermolecular interactions, including molecular recognition interactions between a mesogenic host and nonmesogenic additive (dopant), play an important role in defining the physical properties of the liquid crystal phase. Recent studies have shown that the induction of macroscopic chiral properties such as the helical structure of a chiral nematic or smectic C (SmC*) phase, the electroclinic tilt of a chiral smectic A (SmA*) phase, and the spontaneous electric polarization (P_S) of a SmC* phase in a surface-stabilized ferroelectric state (SSFLC) can be understood in terms of molecular recognition between a chiral dopant and an achiral liquid crystal host.[1−3] The design of chiral dopants based on principles of molecular recognition is of particular interest in the case of ferroelectric SmC* liquid crystals, which are used in commercial high-resolution reflective microdisplays,[4] and hold significant potential in nonlinear optics[5] and photonics applications.[6−8]

The performance characteristics of FLC devices, including electrooptical switching time, second-order NLO susceptibility, and photoswitching threshold, often depend on the magnitude of P_S induced by a chiral dopant. Hence, a key aspect of FLC materials research is to understand the relationship between the molecular structure of a chiral dopant and the magnitude of the spontaneous polarization it induces.[2,9−11] This structure−

[†] Queen's University.
[‡] Displaytech, Inc.

(1) (a) Proni, G.; Spada, G. P. *Enantiomer* **2001**, *6*, 171. (b) di Matteo, A.; Todd, S. M.; Gottarelli, G.; Solladié, G.; Williams, V. E.; Lemieux, R. P.; Ferrarini, A.; Spada, G. P. *J. Am. Chem. Soc.* **2001**, *123*, 7842.
(2) Lemieux, R. P. *Acc. Chem. Res.* **2001**, *34*, 845.
(3) Hegmann, T.; Meadows, M. R.; Wand, M. D.; Lemieux, R. P. *J. Mater. Chem.* **2004**, *14*, 185.
(4) (a) Lagerwall, S. T. *Ferroelectric and Antiferroelectric Liquid Crystals*; Wiley-VCH: Weinheim, 1999. (b) Lagerwall, S. T. In *Handbook of Liquid Crystals*; Demus, D., Goodby, J. W., Gray, G. W., Spiess, H. W., Vill, V., Eds.; Wiley-VCH: Weinheim, 1998; Vol. 2B. (c) Walba, D. M. *Science* **1995**, *270*, 250. (d) Clark, N. A.; Lagerwall, S. T. In *Ferroelectric Liquid Crystals: Principles, Properties and Applications*; Goodby, J. W., Blinc, R., Clark, N. A., Lagerwall, S. T., Osipov, M. A., Pikin, S. A., Sakurai, T., Yoshino, K., Zeks, B., Eds.; Gordon and Breach: Philadelphia, 1991; pp 409−452. (e) Dijon, J. In *Liquid Crystals: Applications and Uses*; Bahadur, B., Ed.; World Scientific: Singapore, 1990; Vol. 1, Chapter 13.
(5) (a) Walba, D. M.; Xiao, L.; Keller, P.; Shao, R.; Link, D.; Clark, N. A. *Pure Appl. Chem.* **1999**, *71*, 2117. (b) Walba, D. M.; Dyer, D. J.; Sierra, T.; Cobben, P. L.; Shao, R. F.; Clark, N. A. *J. Am. Chem. Soc.* **1996**, *118*, 1211. (c) Walba, D. M.; Ros, M. B.; Clark, N. A.; Shao, R. F.; Robinson, M. G.; Liu, J. Y.; Johnson, K. M.; Doroski, D. *J. Am. Chem. Soc.* **1991**, *113*, 5471.
(6) Crossland, W. A.; Wilkinson, T. D. In *Handbook of Liquid Crystals*; Demus, D., Goodby, J. W., Gray, G. W., Spiess, H.-W., Vill, V., Eds.; Wiley-VCH: Weinheim, 1998; Vol. 1, p 763.
(7) Ikeda, T.; Kanazawa, A. In *Molecular Switches*; Feringa, B. L., Ed.; Wiley-VCH: Weinheim, 2001; p 363.
(8) Lemieux, R. P. *Chem. Rec.* **2004**, *3*, 288.
(9) Walba, D. M. In *Advances in the Synthesis and Reactivity of Solids*; Mallouck, T. E., Ed.; JAI Press Ltd.: Greenwich, CT, 1991; Vol. 1, p 173.

10.1021/ja054322k CCC: $30.25

property relationship can be expressed in terms of the polarization power δ_p according to eq 1,[12] where x_d is the mole fraction of chiral dopant and P_o is the polarization normalized for variations in tilt angle θ according to eq 2.[13]

$$\delta_p = \left(\frac{dP_o(x_d)}{dx_d}\right)_{x_d \to 0} \quad (1)$$

$$P_o = P_S/\sin\theta \quad (2)$$

The spontaneous polarization is a chiral bulk property; it is either left-handed (negative) or right-handed (positive) depending on the absolute configuration of the chiral dopant.[9] At the microscopic level, the origins of P_S can be understood in terms of asymmetric conformational energy profiles for polar functional groups sterically coupled to a stereogenic center, which results in the net orientation of transverse molecular dipoles in one direction along the polar C_2 axis of the SmC* phase. Empirical and semiempirical structure−property relationships based on conformational analyses of such stereopolar units are well established for dopants with chiral side-chains, which represent the vast majority of chiral dopants found in SmC* formulations.[9−11] In general, the polarization power of these compounds is invariant with respect to the structure of the SmC liquid crystal host, which is consistent with the Boulder model for the molecular origins of P_S. According to this model, the SmC phase is considered to be a supramolecular host, and the conformational and orientational ordering of a chiral dopant is modeled by a mean field potential which qualitatively behaves like a binding site analogous to that described in host−guest chemistry.[9,10] The binding site is C_{2h} symmetric and has a zigzag shape that is assumed to be invariant with respect to the host structure. To a first approximation, the Boulder model assumes that a chiral dopant plays the role of a "passive" guest, which adopts a conformation that best fits the achiral binding site of the SmC host.

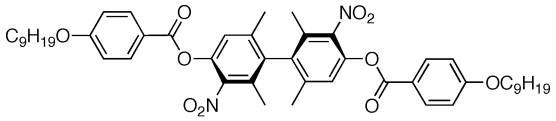

(*R*)-**1**

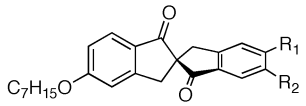

(*R*)-**2**: $R_1 = OC_7H_{15}$, $R_2 = H$
(*R*)-**3**: $R_1 = H$, $R_2 = OC_7H_{15}$

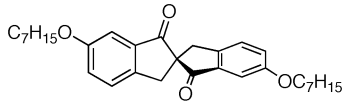

(*R*)-**4**

Less conventional dopants with chiral cores induce spontaneous polarizations that tend to vary significantly with the structure of the SmC host.[2,14,15] This host effect may be viewed as a manifestation of molecular recognition via core−core interactions with the host molecules that cannot be achieved with conventional dopants due to the higher degree of conformational disorder among side-chains in the diffuse layer structure of the SmC phase.[16,17] In other words, the assumption of a shape invariance for the binding site in the original Boulder model appears to break down in the case of dopants with chiral cores. For example, we have shown that dopants such as (*R*)-**1** exhibit remarkably high polarization powers, up to 1738 nC/cm^2, in achiral SmC hosts with a complementary phenylpyrimidine core structure in which the atropisomeric core can propagate its chirality through core−core interactions with surrounding host molecules.[18] The resulting chiral perturbations are thought to cause a chiral distortion of the binding site topography that enhances the polar order of the dopant as a feedback effect (chirality transfer feedback, CTF).[2] We recently measured the effect of chiral perturbations exerted by **1** on the polarization power of a chiral probe molecule (**MDW950**, vide infra).[19] The results showed that the polarization power of the probe decreases by a factor of 0.18 in the presence of (*R*)-**1** and increases by a factor of 1.4 in the presence of (*S*)-**1**, which is consistent with long-range chiral perturbations influencing the conformational distribution of the probe.

Despite the orientational and conformational ordering imposed by the binding site of the SmC host, molecular modeling suggests that the biphenyl core of (*R*)-**1** can rotate almost freely with respect to the ester side-chains (Figure 1) and that the intrinsic conformational bias (i.e., neglecting all intermolecular interactions with host molecules) favoring one orientation of the core dipole moment along the polar axis ($\mu_\perp$) is very small, on the order of 1 kcal/mol.[21] Hence, we postulated that it may be possible to achieve even higher polarization powers by designing dopants with polar chiral cores with high aspect ratio that are conformationally more restricted when confined to the zigzag binding site of the SmC host. In this paper, we report our first implementation of this approach with a series of dopants with an axially chiral 2,2′-spirobiindan-1,1′-dione core, (*R*)-**2**−**4**.[22] As expected, the polarization power varies with the structure of the SmC host, and it also varies with the relative positions of the alkoxy side-chains. These results are rationalized in terms of an equilibrium between conformations of opposite polarities which are energetically equivalent in the gas phase, but should

(10) (a) Glaser, M. A.; Clark, N. A.; Walba, D. M.; Keyes, M. P.; Radcliffe, M. D.; Snustad, D. C. *Liq. Cryst.* **2002**, *29*, 1073. (b) Glaser, M. A. In *Advances in the Computer Simulations of Liquid Crystals*; Zannoni, C., Pasini, P., Eds.; Kluwer: Dordrecht, 1999; p 263.
(11) Goodby, J. W. In *Ferroelectric Liquid Crystals: Principles, Properties and Applications*; Goodby, J. W., Blinc, R., Clark, N. A., Lagerwall, S. T., Osipov, M. A., Pikin, S. A., Sakurai, T., Yoshino, K., Zeks, B., Eds.; Gordon & Breach: Philadelphia, 1991; p 99.
(12) Siemensmeyer, K.; Stegemeyer, H. *Chem. Phys. Lett.* **1988**, *148*, 409.
(13) Kuczynski, W.; Stegemeyer, H. *Chem. Phys. Lett.* **1980**, *70*, 123.
(14) Osipov, M. A.; Stegemeyer, H.; Sprick, A. *Phys. Rev. E* **1996**, *54*, 6387.
(15) Stegemeyer, H.; Meister, R.; Hoffmann, U.; Sprick, A.; Becker, A. *J. Mater. Chem.* **1995**, *5*, 2183.
(16) Tschierske, C. *J. Mater. Chem.* **1998**, *8*, 1485.
(17) For a related example of molecular recognition via core−core interactions in SmC* liquid crystals, see: (a) Yoshizawa, A.; Nishiyama, I. *Mol. Cryst. Liq. Cryst.* **1995**, *260*, 403. (b) Nishiyama, I.; Ishizika, H.; Yoshizawa, A. *Ferroelectrics* **1993**, *147*, 193.
(18) Vizitiu, D.; Lazar, C.; Halden, B. J.; Lemieux, R. P. *J. Am. Chem. Soc.* **1999**, *121*, 8229.
(19) Hartley, C. S.; Lazar, C.; Wand, M. D.; Lemieux, R. P. *J. Am. Chem. Soc.* **2002**, *124*, 13513.
(20) According to the physics convention, the spontaneous polarization points from the negative to the positive end of a dipole, which is opposite to that used in chemistry. A positive P_S corresponds to the cross product of the director and the layer normal, $\mathbf{n} \times \mathbf{z}$, respectively.[9]
(21) Vizitiu, D.; Lazar, C.; Radke, J. P.; Hartley, C. S.; Glaser, M. A.; Lemieux, R. P. *Chem. Mater.* **2001**, *13*, 1692.
(22) For a preliminary communication, see: Boulton, C. J.; Sutherland, J. J.; Lemieux, R. P. *J. Mater. Chem.* **2003**, *13*, 644.

Scheme 1 [a]

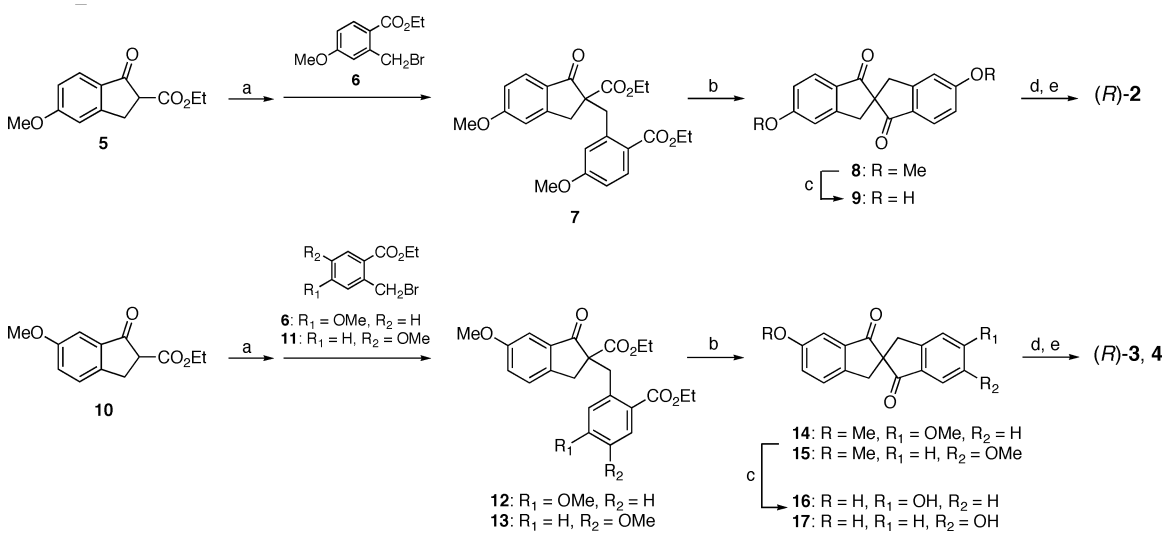

[a] Reagents and conditions: (a) NaH, DMF, 60 °C; (b) 70% aqueous H_2SO_4, 90 °C; (c) $AlCl_3$, toluene, reflux; (d) 1-bromoheptane, K_2CO_3, acetone, reflux; (e) semiprep HPLC resolution, Daicel Chiralpak AS column, 2% EtOH/hexanes, 3 mL/min.

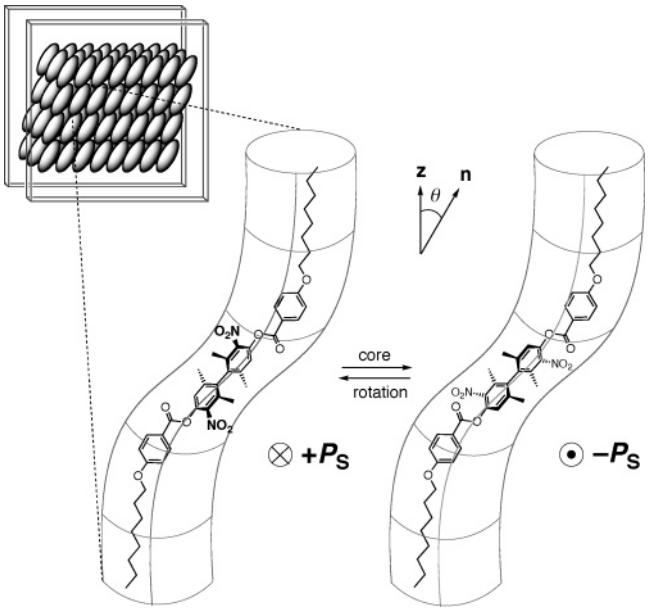

Figure 1. Rotation of the biphenyl core about the two ester C−O single bonds of dopant (*R*)-**1** confined to the binding site of the Boulder model in an idealized zigzag conformation. The chiral SmC* phase is represented in a surface-stabilized ferroelectric state (SSFLC); the layer normal **z** and the director **n** are in the plane of the page and form a tilt angle θ. The spontaneous polarization P_s is coincident with the C_2 symmetry axis of the SSFLC, which is normal to the plane of the page. The sign of P_S conforms to the physics convention.[20]

have different steric demands in the condensed phase when confined to the binding site of the SmC host.

Results

Synthesis. The three chiral dopants were synthesized as racemic mixtures using a strategy reported by Nieman and Keay for the synthesis of 2,2′-spirobiindan-1,1′-dione.[23] As shown in Scheme 1, reactions of the enolate of either indanonecarboxylate **5** or **10** with the appropriate ethyl 2-(bromomethyl)benzoate **6** or **11** gave the substitution products **7**, **12**, and **13** in 81−99% yields. Acid-catalyzed hydrolysis was followed by decarboxylation and cyclization in situ to give the racemic dimethoxyspirobiindandiones **8**, **14**, and **16** in 54−82% yields. Demethylation with $AlCl_3$ and alkylation of the resulting diols with 1-bromoheptane gave the racemic dopants **2**−**4** in 46−84% yields. The enantiomers of **2**−**4** were resolved by semiprep chiral stationary phase HPLC using a Daicel Chiralcel AS column and 2% ethanol/hexanes as the mobile phase. The resolved compounds were recrystallized from hexanes prior to doping in the liquid crystal hosts.

In each case, the absolute configuration of the first HPLC eluant was assigned as (*R*) by the exciton chirality method using circular dichroism (CD) spectroscopy.[24] Previous work by Schlögl has shown that the absolute configurations of 2,2′-spirobiindan-1,1′-dione and 5,5′-disubstituted 2,2′-spirobiindan derivatives can be assigned with a reasonable degree of certainty according to the sign of split Cotton effects corresponding to ^1L_a and ^1L_b exciton couplets.[25,26] As shown in Figure 2, the CD spectra of the first eluants of dopants **2**−**4** feature strong positive split Cotton effects at wavelengths corresponding to UV absorption bands at λ_{max} = 219, 221, and 222 nm, respectively. Weaker positive split Cotton effects are also observed at longer wavelengths in the spectra of **2** and **4**. The electronic transitions of the model compounds 5- and 6-methoxyindan-1-one were calculated using the semiempirical ZINDO method (Figure 3).[27] In each case, the calculations predict a pair of $\pi-\pi^*$ transitions with excitation wavelengths in the 210−220 nm range, with one of the two transition dipole

(23) Nieman, J. A.; Keay, B. A. *Tetrahedron: Asymmetry* **1995**, *6*, 1575.

(24) (a) Berova, N.; Nakanishi, K. In *Exciton Chirality Methods: Principles and Applications*; Berova, N., Nakanishi, K., Woody, R. W., Eds.; Wiley-VCH: New York, 2000. (b) Harada, N.; Nakanishi, K. *Circular Dichroic Spectroscopy: Exciton Coupling in Organic Photochemistry*; University Science Books: New York, 1983.

(25) Falk, H.; Fröstl, W.; Hofer, O.; Schlögl, K. *Monatsh. Chem.* **1974**, *105*, 598.

(26) Langer, E.; Lehner, H.; Neudeck, H.; Schlögl, K. *Monatsh. Chem.* **1978**, *109*, 987.

(27) (a) Zerner, M. C. In *Review in Computational Chemistry*; Lipkowitz, K. B., Boyd, D. B., Eds.; VCH: New York, 1991; pp 313−366. (b) Ridley, J. E.; Zerner, M. C. *Theor. Chim. Acta* **1973**, *32*, 111.

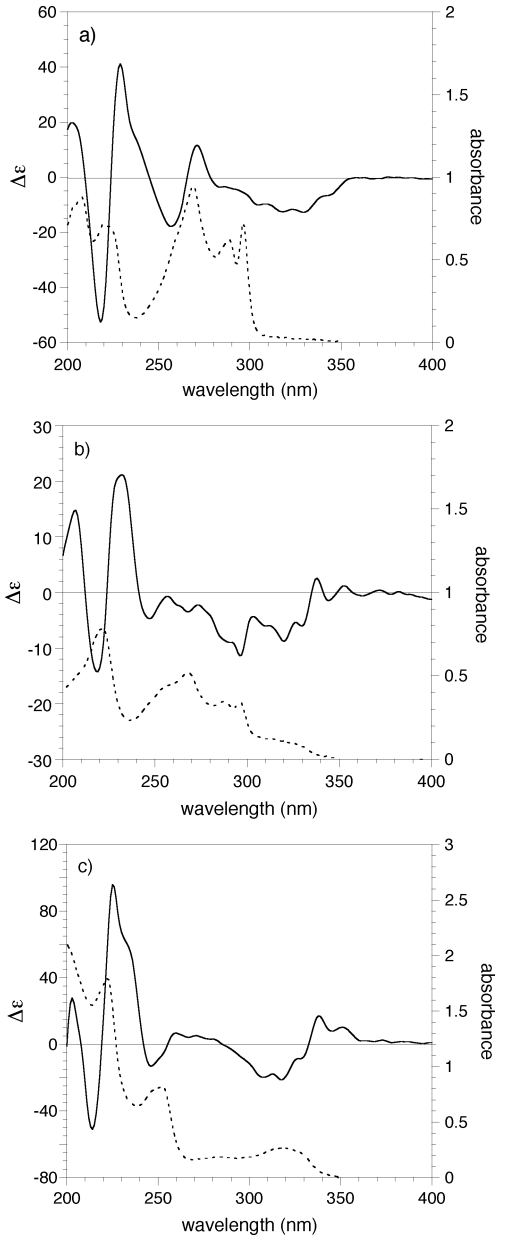

Figure 2. Circular dichroism (−) and UV (- - -) absorption spectra of (a) dopant (*R*)-**2** (1.7×10^{-5} M), (b) dopant (*R*)-**3** (2.0×10^{-5} M), and (c) dopant (*R*)-**4** (1.4×10^{-5} M) in hexanes.

moments having a large component normal to the helical axis of the 2,2′-spirobiindan-1,1′-dione chromophore, which is consistent with the strong split Cotton effects observed in that spectral region. According to exciton chirality rules, a positive split Cotton effect results from coupling of transition dipoles that describe a right-handed (*P*) helix, which corresponds to the (*R*) absolute configuration in **2**−**4**.

To confirm the stereochemical assignments, the second HPLC eluant of **4** was reduced stereoselectively to the *cis*/*trans*-diol **18** in 74% yield using $LiAlH_4$,[28] and then converted to the bis-*p*-dimethylaminobenzoate derivative **19** in 58% yield (Scheme 2). The unambiguous assignment of the cis/trans configuration in **18** was based on the ^1H NMR spectrum,

(28) Dynesen, E. *Acta Chem. Scand., Ser. B* **1975**, *29*, 77.

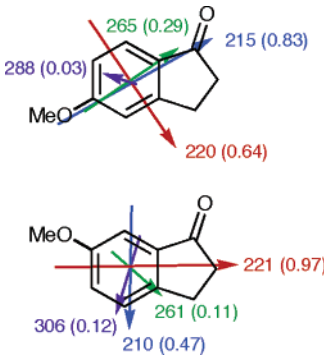

Figure 3. Transition dipole moments ($\pi-\pi^*$) with the corresponding excitation wavelengths and oscillator strengths (in parentheses) of 5-methoxyindan-1-one (top) and 6-methoxyindan-1-one (bottom) calculated using the semiempirical ZINDO method.

Scheme 2 [a]

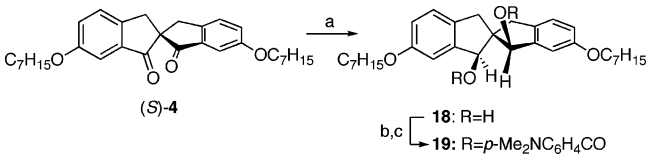

[a] Reagents and conditions: (a) $LiAlH_4$, THF, 25 °C; (b) NaH, THF, 25 °C; (c) 1-(4-*N*,*N*-dimethylaminobenzoyl)benzotriazole, THF, reflux.

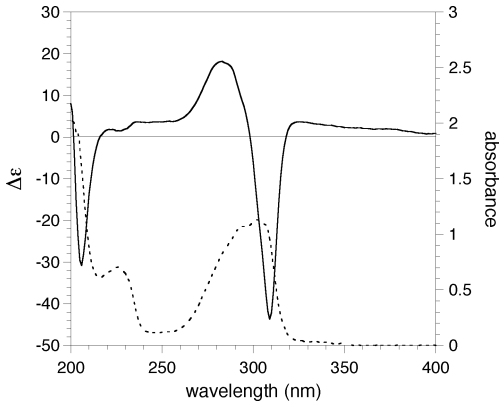

Figure 4. Circular dichroism (−) and UV (- - -) absorption spectra of compound **19** (2.0×10^{-5} M) in hexanes.

which showed two peaks for the methine protons at 4.94 and 5.51 ppm. In this configuration, the transition dipoles of the two *p*-dimethylaminobenzoate groups form an angle of ca. 90°, which is optimum for chiral exciton coupling.[24,29] As shown in Figure 4, the CD spectrum of **19** shows a strong negative split Cotton effect centered at 298 nm, which indicates that the two benzoate groups describe a left-handed (*M*) helix corresponding to the (*S*) absolute configuration in **4**. This result confirms the assignment of the (*R*) configuration to the firstHPLC eluant of **4** and strongly supports the same assignments made for **2** and **3**.

Dopant−Host Compatibility. The compounds (*R*)-**2**−**4** were doped in the liquid crystal hosts **PhP1**, **PhB**, **DFT**, and **NCB76**, which exhibit I−N−A−C phase sequences. We observed significant differences in solubility between the three dopants in the SmC phases of **PhP1**, **PhB**, and **DFT**, which is

(29) This approach was used to determine the absolute configuration of unsubstituted 2,2′-spirobiindan-1,1′-dione: Harada, N.; Ai, T.; Uda, H. *J. Chem. Soc., Chem. Commun.* **1982**, 232.

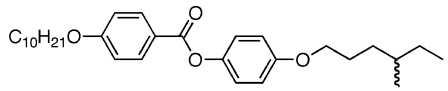

PhB: Cr 35 SmC 70.5 SmA 72 N 75 I

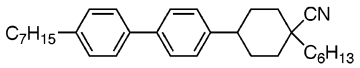

NCB76: Cr 66 (SmG 55) SmC 73 SmA 117 N 125 I

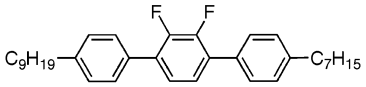

DFT: Cr 49 SmC 77 SmA 93 N 108 I

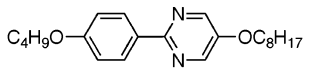

PhP1: Cr 58 SmC 85 SmA 95 N 98 I

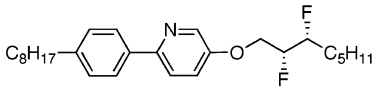

MDW950

noteworthy in light of molecular modeling predictions that the three dopants should have similar molecular shapes and conformational distributions (vide infra). Solubility limits were estimated by polarized microscopy based on the observation of persistent biphasic SmC*/isotropic domains at 10 K below the Curie point of a given mixture ($T-T_C = -10$ K). The solubility limits in **PhP1**, **PhB**, and **DFT** range from ca. 25 to 30 mol % for the 5,5′-dialkoxy derivative (*R*)-**2**, 10 to 15 mol % for the 5,6′-dialkoxy derivative (*R*)-**3**, and only 3 to 5 mol % for the 6,6′-dialkoxy derivative (*R*)-**4**. The solubility limits are higher in **NCB76**: in excess of 25 mol % for both (*R*)-**2** and **3**, and 10 mol % for (*R*)-**4**. The phase diagrams in Figure 5 show that addition of (*R*)-**2** causes a severe destabilization of the SmC phase formed by **PhP1**, and a more moderate destabilization of the SmC phase formed by **PhB** and **DFT**. Interestingly, addition of (*R*)-**2** has virtually no effect on the SmA−C phase transition temperature of **NCB76**, which suggests that the binding site of this host provides a good fit for the chiral dopant. A comparison of phase diagrams for mixtures of (*R*)-**2**, -**3**, and -**4** in **NCB76** reveals a growth in biphasic regions and increasing mesophase destabilization going from the 5,5′- to the 6,6′-dialkoxy derivative, which are consistent with the trend in solubility limit established by polarized microscopy.

Dopant−host compatibility was also assessed by ^{2}H NMR spectroscopy using the racemic dopants (*RS*)-**2**-d_4, **3**-d_4, and **4**-d_4 with dideuterated side-chains ($-OCD_2C_6H_{13}$), which were mixed in the four liquid crystal hosts below the solubility limits established by polarized microscopy. In an anisotropic liquid crystal phase, the interaction of the quadrupolar moment of a deuterium nucleus with the electric field gradient tensor produces a quadrupolar doublet with a splitting $\Delta\nu_Q$ that is directly proportional to the orientational order parameter of the C−D bond. Hence, ^{2}H NMR spectroscopy has been used extensively to measure the order parameters of deuterated mesogens[30] and to characterize the local environment of nonmesogenic dopants in liquid crystal hosts.[31,32] As shown in Figure 6, ^{2}H NMR spectra of (*RS*)-**2**-d_4 (10 mol %) in each of the four hosts at $T-T_C = -10$ K feature only quadrupolar doublets with $\Delta\nu_Q$ values on the order of 60−70 kHz, which indicates that all of the dopant molecules in these mixtures reside in a liquid crystalline environment. Remarkably, the ^{2}H NMR spectra of (*RS*)-**3**-d_4 and (*RS*)-**4**-d_4 in **PhP1** (10 and 2.9 mol %, respectively) feature an isotropic singlet together with a weak quadrupolar doublet, which suggests that the dopant molecules reside primarily in isotropic microdomains that cannot be observed by polarized microscopy.[32] No isotropic singlet was observed with the other liquid crystal mixtures containing (*RS*)-**3**-d_4 or (*RS*)-**4**-d_4. These results suggest that all three dopants form homogeneous mixtures with **PhB**, **NCB76**, and **DFT** below the solubility limits established by polarized microscopy.

Most of the spectra feature pairs of quadrupolar doublets, which are well resolved in the spectra of (*RS*)-**4**-d_4 ($\Delta\Delta\nu_Q$ = 24−30 kHz), but only partially resolved in the spectra of (*RS*)-**2**-d_4 ($\Delta\Delta\nu_Q$ = 0−7 kHz). The spectra of (*RS*)-**3**-d_4 are more complex due to its unsymmetrical configuration, but appear to combine the spectral features of the other two dopants. There are two likely explanations for the presence of quadrupolar doublet pairs: (i) a partitioning of the dopant between two different mesophases, or (ii) a chiral perturbation of the local environment of the dopant causing the methylene deuterons to become nonequivalent. The first possibility was ruled out based on observations of doublet pairs with smaller quadrupolar splittings in the nematic phase of the 10% mixtures in **DFT** (Figure 6), as well as in the nematic phase of a 3 mol % mixture of (*RS*)-**4**-d_4 in 4-cyano-4′-pentyloxybiphenyl, which forms only a nematic phase (see Supporting Information). With respect to the second possibility, Samulski showed that the enantiotopic methylene deuterons of perdeuterated benzyl alcohol become diastereotopic when dissolved in a chiral nematic liquid crystal formed by a solution of poly-γ-benzyl-L-glutamate (PBLG) in CH_2Cl_2.[33] This has proven to be a general effect for enantiotopic CD_2 groups in molecules such as perdeuterated butanol, octanol, and 4-cyano-4′-pentylbiphenyl dissolved in PBLG, which was attributed to a difference in orientational order parameter of the two C−D bonds due to a reduction in symmetry of the anisotropic solute−solvent interaction potential.[34] In the case of (*RS*)-**2**−**4**-d_4, the methylene deuterons are formally diastereotopic, but they should be undistinguishable in an achiral liquid crystal host given their distance to the stereogenic center, if the dopant molecules are passive. However, a chiral perturbation exerted by the dopant on the liquid crystal host via core−core interactions could create the local chiral environment necessary

(30) Dong, R. Y. In *Encyclopedia of Nuclear Magnetic Resonance*; Grant, D. M., Harris, R. K., Eds.; John Wiley & Sons: 1996; Vol. 4, pp 2752−2760.
(31) (a) Workentin, M. S.; Leigh, W. J. *J. Phys. Chem.* **1992**, *96*, 9666. (b) Workentin, M. S.; Fahie, B. J.; Leigh, W. J. *Can. J. Chem.* **1991**, *69*, 1435. (c) Workentin, M. S.; Leigh, W. J.; Jeffrey, K. R. *J. Am. Chem. Soc.* **1990**, *112*, 7329. (d) Fahie, B. J.; Mitchell, D. S.; Leigh, W. J. *Can. J. Chem.* **1989**, *67*, 148. (e) Fahie, B. J.; Mitchell, D. S.; Workentin, M. S.; Leigh, W. J. *J. Am. Chem. Soc.* **1989**, *111*, 2916.
(32) (a) Vlahakis, J. Z.; Lemieux, R. P. *J. Mater. Chem.* **2004**, *14*, 1486. (b) Maly, K. E.; Wu, G.; Lemieux, R. P. *Liq. Cryst.* **2001**, *28*, 457.
(33) Czarniecka, K.; Samulski, E. T. *Mol. Cryst. Liq. Cryst.* **1981**, *63*, 205.
(34) (a) Emsley, J. W.; Lesot, P.; Courtieu, J.; Merlet, D. *Phys. Chem. Chem. Phys.* **2004**, *6*, 5331. (b) Merlet, D.; Loewenstein, A.; Smadja, W.; Courtieu, J.; Lesot, P. *J. Am. Chem. Soc.* **1998**, *120*, 963. (c) Meddour, A.; Canet, I.; Loewenstein, A.; Péchiné, J. M.; Courtieu, J. *J. Am. Chem. Soc.* **1994**, *116*, 9652.

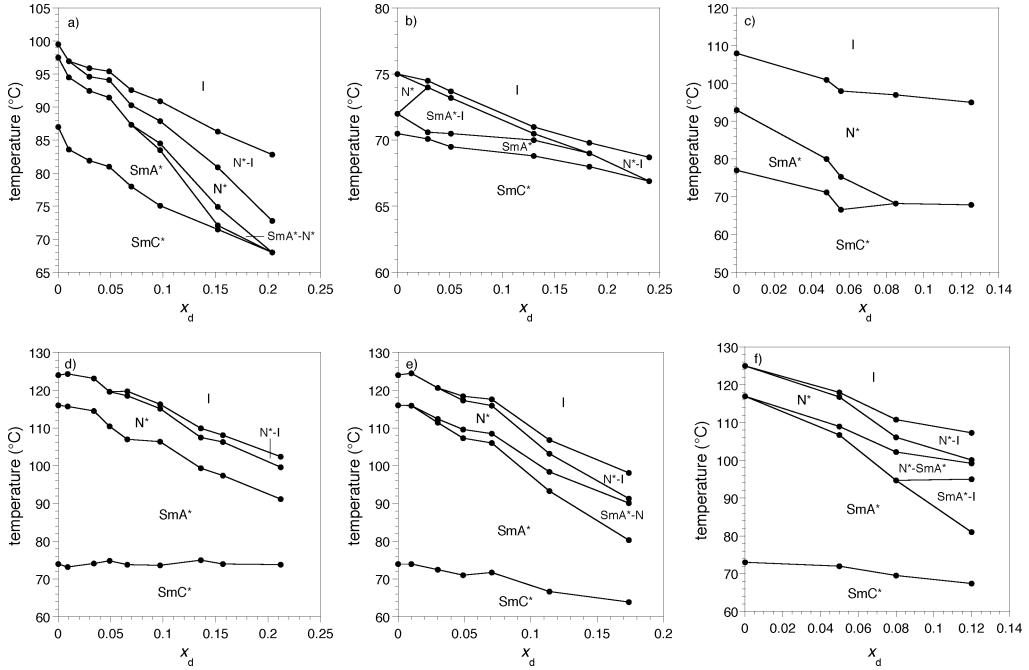

Figure 5. Partial phase diagrams for mixtures of (a) (*R*)-**2** in **PhP1**, (b) (*R*)-**2** in **PhB**, (c) (*R*)-**2** in **DFT**, (d) (*R*)-**2** in **NCB76**, (e) (*R*)-**3** in **NCB76**, and (f) (*R*)-**4** in **NCB76**. The phase transition temperatures were measured by polarized microscopy on cooling; x_d is the dopant mole fraction.

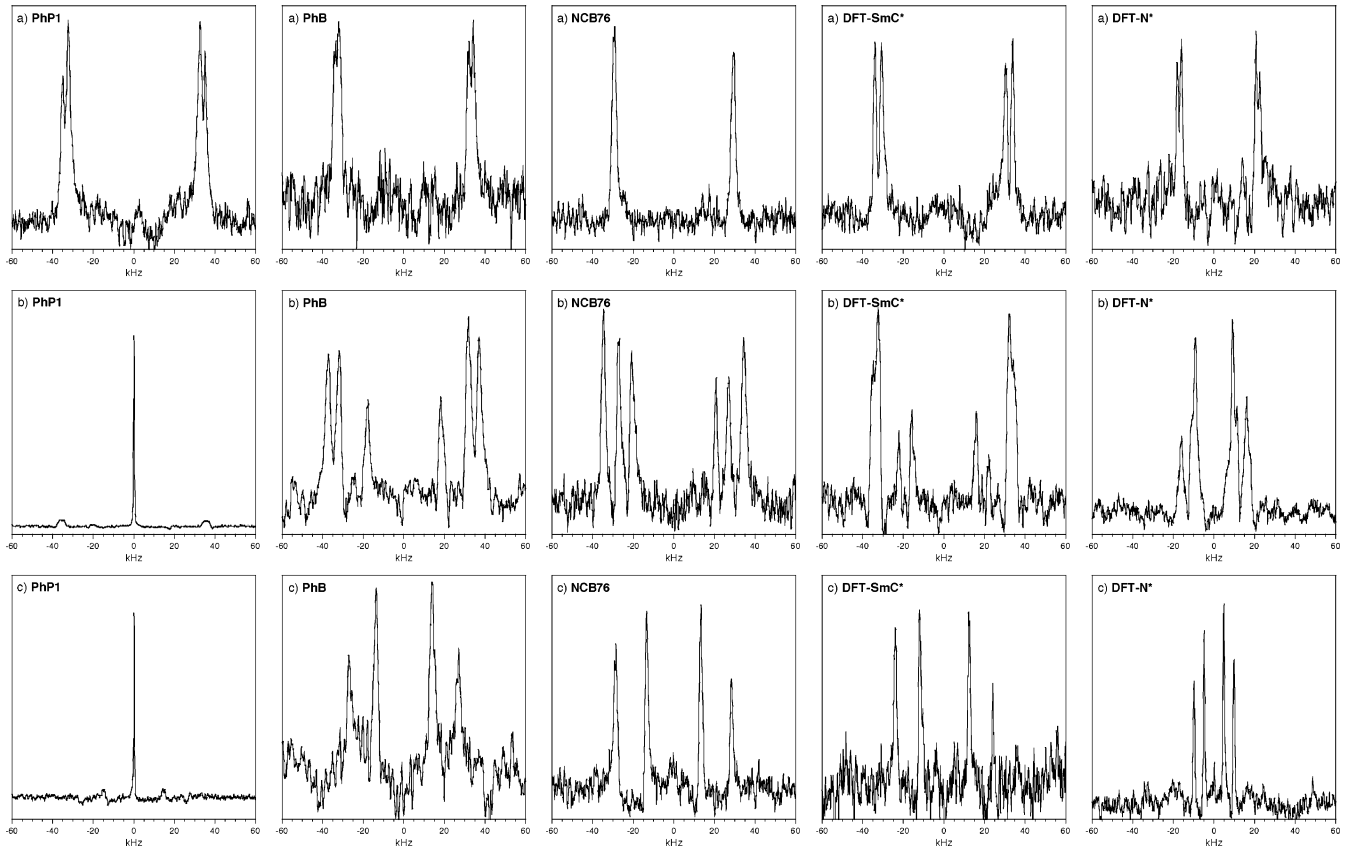

Figure 6. ^{2}H NMR spectra (92.13 MHz) of (a) 10 mol % mixtures of (*RS*)-**2**-d_4 in the four liquid crystal hosts, (b) 10 mol % mixtures of (*RS*)-**3**-d_4 in the four liquid crystal hosts, and (c) mixtures of (*RS*)-**4**-d_4 in the four liquid crystal hosts at the following concentrations: 2.6 mol % (**PhP1**), 3 mol % (**PhB**), 5 mol % (**NCB76**), and 3 mol % (**DFT**). Each spectrum was taken in the SmC* phase at $T-T_C = -10$ K, except those in the fifth column, which were taken in the N* phase.

to make the pro-*R* and pro-*S* deuterons nonequivalent in a ^{2}H NMR spectrum. In such cases, the difference in $\Delta\nu_Q$ between two quadrupolar doublets ($\Delta\Delta\nu_Q$) should reflect the degree of chiral perturbation exerted by the dopant on the liquid crystal host. In the host **DFT**, we observed a decrease in $\Delta\Delta\nu_Q$ going from the SmC* to the N* phase, which is consistent with a weakening of chiral perturbations by the dopant due to a lack of positional order (core−core correlation) in the nematic phase. According to this rationale, the combined results of the ^{2}H NMR experiments suggest that the 6,6′-dialkoxy derivative (*R*)-**4** exerts

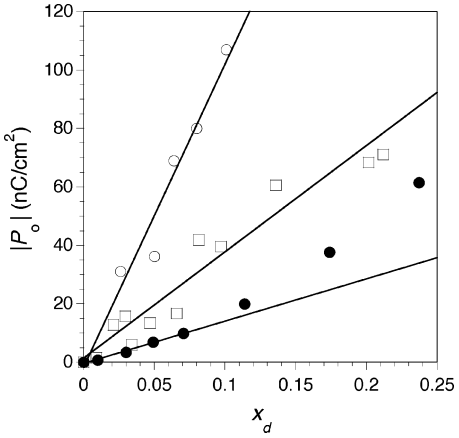

Figure 7. Absolute value of reduced polarization $|P_o|$ versus dopant mole fraction x_d for dopants (*R*)-**2** (□), (*R*)-**3** (●), and (*R*)-**4** (○) in **NCB76** at $T-T_C = -10$ K.

Table 1. Polarization Powers δ_p of (*R*)-**2**, -**3**, and -**4** in the Hosts **PhP1**, **PhB**, **NCB76**, and **DFT** at $T-T_C = -10$ K

	δ_p (nC/cm^2)[a,b]			
dopant	PhP1	PhB	NCB76	DFT
(*R*)-**2**	749 ± 35 (+)	460 ± 13 (+)	363 ± 30 (+)	21 ± 3 (+)
(*R*)-**3**	>11 (+)	130 ± 7 (−)	144 ± 7 (−)	220 ± 5 (−)
(*R*)-**4**	>160 (−)	79 ± 9 (−)	1037 ± 100 (−)	285 ± 26 (−)

[a] Sign of polarization in parentheses. [b] Uncertainty is ± standard error of least-squares fit.

stronger chiral perturbations in the SmC* phase than the 5,5′-dialkoxy derivative (*R*)-**2**.

Polarization Power Measurements. Homogeneous mixtures of (*R*)-**2**, -**3**, and -**4** in the four liquid crystal hosts were aligned as SSFLC films using commercial ITO glass cells with rubbed polyimide surfaces and a cell gap of 4 μm. Spontaneous polarizations (P_S) and tilt angles (θ) were measured in the SmC* phase at $T-T_C = -10$ K by the triangular wave method,[35] and the corresponding P_o values were calculated using eq 2. A minimum of five different mixtures were prepared for each dopant/host combination (except for (*R*)-**4** in **PhP1** due to low solubility), and the resulting P_o values were plotted as a function of the dopant mole fraction x_d. The plots gave good least-squares fits ($R^2 = 0.928-0.998$) except for (*R*)-**3** in **NCB76**, which gave a plot showing a positive deviation from linearity at $x_d > 0.10$ (Figure 7). The polarization power values were derived from the P_o versus x_d plots using eq 1 and are listed in Table 1; δ_p values for (*R*)-**3** and -**4** in **PhP1** are given as lower limits based on the ^{2}H NMR findings that the dopants reside primarily in isotropic microdomains. The sign of P_S along the polar axis was assigned from the relative configuration of the electric field and the switching position of the SSFLC film according to the established convention.[9] As shown in Table 1, the polarization power of (*R*)-**2** is uniformly positive and varies significantly with the host structure. Conversely, the polarization power of (*R*)-**4** is uniformly negative and shows a different trend in host dependence, with the highest δ_p value of −1037 nC/cm^2 obtained in **NCB76**. The unsymmetrical dopant (*R*)-**3** seems to behave as a hybrid of the two symmetrical isomers (*R*)-**2** and -**4**. Its polarization power is lower, on average, and the sign of P_S is not the same in all four hosts, which is consistent with competing conformational biases (vide infra).

(35) Miyasato, K.; Abe, S.; Takezoe, H.; Fukuda, A.; Kuze, E. *Jpn. J. Appl. Phys.* **1983**, *22*, L661.

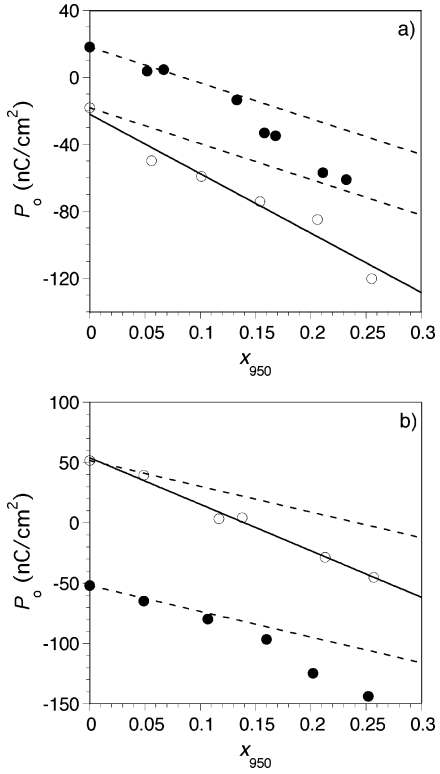

Figure 8. Reduced polarization P_o versus mole fraction of **MDW950** in **NCB76** at $T-T_C = -10$ K: (a) in the presence of (*R*)-**2** (●) and (*S*)-**2** (○) at $x_2 = 0.05$ and (b) in the presence of (*R*)-**4** (●) and (*S*)-**4** (○) at $x_4 = 0.05$. The slope of the dashed lines (−214 nC/cm^2) corresponds to the polarization power of **MDW950** in the absence of the chiral dopant.

Probe Experiments. Previous work has shown that chiral perturbations exerted by dopants with chiral cores can be detected in the SmC* phase using the Displaytech dopant **MDW950** as probe.[19] These experiments are based on the assumption that any long-range perturbation exerted by a chiral dopant should affect the conformational equilibrium of the probe and, consequently, its polarization power (δ_{probe}). To determine whether a perturbation is chiral, δ_{probe} is measured in the presence of each enantiomer of the chiral dopant; if they exert chiral perturbations, the two enantiomers should have different effects on δ_{probe}. Hence, to test the hypothesis that (*R*)-**4** may exert stronger chiral perturbations in the SmC* phase than (*R*)-**2**, we performed a series of probe experiments with **MDW950** in the host **NCB76**, in which the largest difference in $\Delta\Delta\nu_Q$ between (*RS*)-**2**-d_4 (0 kHz) and (*RS*)-**4**-d_4 (30 kHz) was observed. The reduced polarization induced by **MDW950** was measured as a function of its mole fraction x_{950} in the presence of the (*R*) and (*S*) enantiomers of each chiral dopant at a constant mole fraction of 0.05 (5 mol %). As shown in Figure 8, the resulting plots of P_o versus x_{950} are shifted up and down the *y*-axis by values equal to P_o induced by the (*R*) and (*S*) enantiomers of (*R*)-**2** and -**4** in the absence of the probe. The results show that the polarization power of **MDW950** (δ_{950}) increases by the same amount, within error, in the presence of either (*S*)-**2** or (*S*)-**4** ($\delta_{950} = -355 \pm 37$ and -386 ± 19 nC/cm^2, respectively). The plots obtained in the presence of (*R*)-**2** and (*R*)-**4** also indicate an increase in δ_{950}, but they both appear to deviate from linearity. These results suggest that the two dopants exert similar long-range perturbations in **NCB76**, which are, at best, weakly chiral in comparison to the chiral perturba-

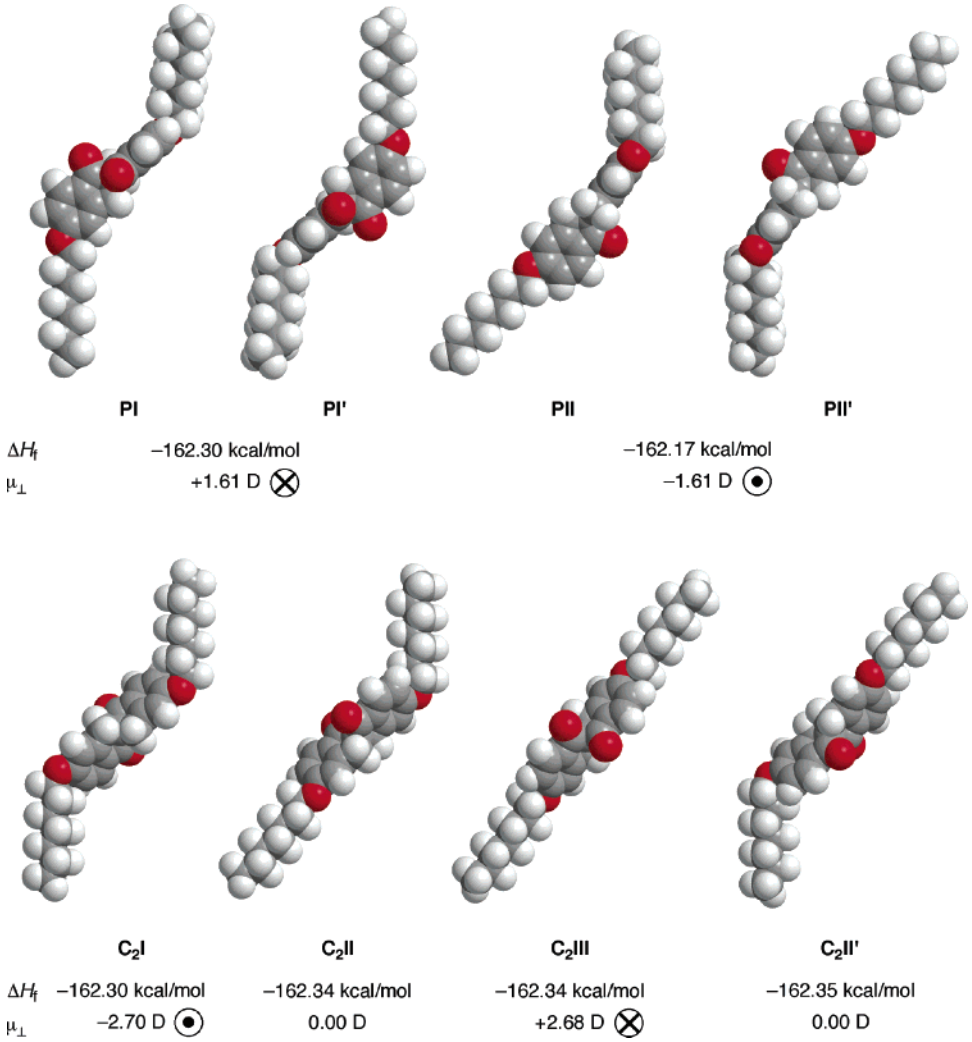

Figure 9. Space-filling models showing conformational distributions of dopant (*R*)-**2** as side-on views with the spirobiindandione core in planar and C_2 orientations. The heats of formation (ΔH_f) and dipole moments along the polar axis ($\mu_\perp$) were calculated for each minimized structure at the AM1 level. The $\mu_\perp$ vectors point from negative to positive according to the physics convention.[20] The chiral axis of the spirobiindandione core is congruent with the tilt plane (plane of the page), and the polar axis is normal to the plane of the page.

tions exerted by (*R*)-**1** in **PhP1** according to a similar probe experiment (vide supra).[19]

Conformational Analyses. To understand the molecular origins of the polarization induced by (*R*)-**2**−**4** and the dependence of δ_p on the structure of the host, conformational analyses of the three dopants are carried out at the AM1 level within the framework of the Boulder model; that is, the chiral dopants were considered to be passive guests that conform to the achiral binding site of the host in the SmC phase (see Figure 1). In this model, we assume that each dopant adopts a zigzag conformation with the core more tilted than the side-chains, that the alkoxy side-chains are fully extended with the methylene groups in anti conformations, and that the ether linking groups are coplanar with the aromatic rings. The calculations suggest that the three dopants are in equilibrium between two conformations with different core orientations, as shown in Figure 9. In one conformation (**P**), the plane of one indanone fragment is congruent with the tilt plane defined by **n** and **z**; in the other conformation ($\mathbf{C_2}$), the C_2 axis of the core is coincident with the polar axis. An analysis of conformational distributions for the two core orientations of (*R*)-**2** reveals a conformational bias that may be responsible for the induced polarization.[36] In each case, the analysis begins with the minimized conformation that best "fits" the zigzag binding site. The core is then rotated by 90° increments about its chiral axis, and each structure is minimized at the AM1 level after the side-chains are rotated to give the closest fit to the zigzag binding site. As shown in Figure 9, two pairs of degenerate **P** conformations are obtained, **PI/I′** and **PII/II′**,[37] with equal but opposite dipole moments along the polar axis ($\mu_\perp$). Although the difference in energy between **PI/I′** and **PII/II′** is insignificant in the gas phase, the Boulder model predicts that **PII/II′** should be disfavored because its bent shape does not conform to the zigzag binding site. Similarly, the conformations $\mathbf{C_2I}$ and $\mathbf{C_2III}$ have equal but opposite dipole

(36) These gas-phase conformational distributions are oversimplifications of complex conformational/orientational hypersurfaces and neglect dopant−host intermolecular interactions, but they do provide a useful basis to understand the molecular origins of P_s.[9] More rigorous analyses based on atomistic molecular dynamics simulations are currently under development: Ghenea, R.; Cann, N. M., unpublished results. A related Monte Carlo molecular simulation method that calculates helical twisting powers based on fully atomistic structures of chiral dopants in a Gay−Berne nematic liquid crystal solvent has recently been reported: Earl, D. J.; Wilson, M. R. *J. Chem. Phys.* **2004**, *120*, 9679.

(37) The two conformations in each degenerate pair can be interconverted by a 180° rotation about the polar axis.

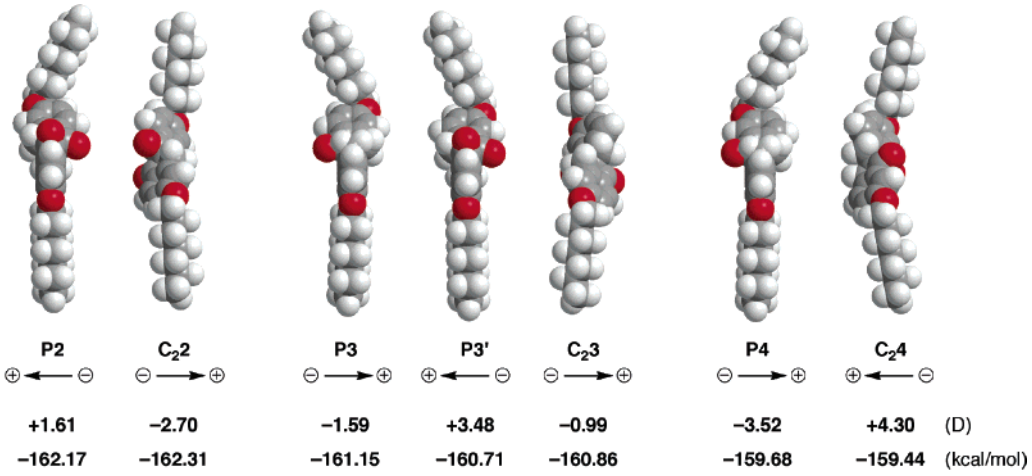

Figure 10. Space-filling models showing minimized zigzag conformations of dopants (*R*)-**2**, -**3**, and -**4** as end-on views with the spirobiindandione core in planar and C_2 orientations. The heats of formation (ΔH_f) and dipole moments along the polar axis ($\mu_\perp$) were calculated for each minimized structure at the AM1 level. The tilt plane is vertical and normal to the plane of the page, and the polar axis is horizontal and in the plane of the page. The $\mu_\perp$ vectors point from negative to positive according to the physics convention.[20]

moments along the polar axis, but the latter is disfavored because of its linear shape. The other two degenerate conformations have no dipole moment along the polar axis and may therefore be neglected. Overall, the analysis suggests that the spontaneous polarization induced by (*R*)-**2** depends on the position of the equilibrium between the zigzag conformations **PI/I′** and **C₂I**, which have dipole moments in opposite directions along the polar axis.

Similar conformational analyses were carried out for (*R*)-**3** and -**4**; the corresponding **P** and **C₂** zigzag conformations are shown in Figure 10 as end-on views along with those of (*R*)-**2**. The conformational distribution of the symmetrical dopant (*R*)-**4** is essentially the same as that of (*R*)-**2**, but predicts an induced polarization of opposite sign. The distribution of the unsymmetrical dopant (*R*)-**3** is more complex; the C_2 core orientation has two degenerate zigzag conformations, and the planar core orientation has two nondegenerate zigzag conformations with $\mu_\perp$ of opposite signs. In each case, alkoxy and carbonyl groups contribute to the dipole moment along the polar axis, either constructively or (partially) destructively, except in the case of conformation **C₂3**, in which the transverse dipole moments of the two carbonyl groups cancel out.

Discussion

The results described herein paint a rather complex picture of the dependence of δ_p on the structure of the dopant and the nature of the liquid crystal host, which includes significant differences in dopant−host compatibility, and in the degree of chiral perturbations exerted by the dopants on the achiral SmC phase. Let us first consider the general trends in sign and magnitude of induced polarization with respect to dopant structure. The 5,5′-dialkoxy dopant (*R*)-**2** induces a positive polarization in all four hosts, whereas the 6,6′-dialkoxy dopant (*R*)-**4** induces a negative polarization in all four hosts, which is consistent with the results of the conformational analysis and suggests that **P** conformations are generally favored over C_2 in the SmC binding site. The δ_p data for the "hybrid" dopant (*R*)-**3** is consistent with a more complex conformational distribution, as predicted by the conformational analysis. The data for (*R*)-**3** may also be rationalized by assuming a predominance of **P** over **C₂**, and that a finer balance between **P3** and **P3′** may be responsible for the polarization inversion.[38]

Results of the probe experiments in **NCB76** suggest that neither (*R*)-**2** nor (*R*)-**4** exert strong, long range chiral perturbations comparable to those exerted by (*R*)-**1** in **PhP1** under the same experimental conditions.[19] However, the ^{2}H NMR experiments strongly suggest that both (*R*)-**3** and -**4** exert short range chiral perturbations that might still influence the conformational distribution of the dopant according to the CTF model. The positive deviation from linearity observed in the P_o versus x_d plot for (*R*)-**3** in **NCB76** at relatively high mole fractions ($x_d > 0.10$) suggests a cooperative effect that is consistent with the CTF model. Unfortunately, we were unable to measure polarizations in that higher mole fraction range with (*R*)-**3** in the other hosts, or with (*R*)-**4** in any host due to solubility limits. On the other hand, the linearity of the P_o versus x_d plots for (*R*)-**2** at mole fractions as high as 0.25, together with the small $\Delta\Delta\nu_Q$ values observed in the corresponding ^{2}H NMR spectra, suggest that (*R*)-**2** exerts very weak, perhaps negligible, chiral perturbations in the four liquid crystal hosts.

If one assumes that the CTF effect does not contribute to the polarization induced by (*R*)-**2**, the dependence of δ_p on the nature of the host may be understood in terms of a shift in the **P**/**C₂** conformational equilibrium that is controlled primarily by a difference in conformational steric demand in the core region of the binding site. If one simplifies the binding site of the Boulder model to three cylindrical sections forming a zigzag shape, steric demand in the core region may be approximated by the distance between atomic coordinates where divergence from the central cylindrical space begins. As shown in Figure 11, this approximation reveals that the core section of the **P** conformation is ca. 1.5 Å shorter than that of the **C₂** conformation, which suggests that the **P**/**C₂** conformational equilibrium should shift toward the **P** conformation (positive $\mu_\perp$) as the core

(38) The reason **P3** would be favored over **P3′** in three of the four hosts remains unclear. In conformation **P3′**, the 6-heptyloxyindanone fragment is oriented perpendicular to the tilt plane, which may be less compatible with the SmC binding site than the 5-heptyloxyindanone fragment in the same orientation. Interestingly, the perpendicular orientation of the 6-heptyloxyindanone fragment is also present in **P4**, but it cannot be avoided, as in (*R*)-**3**, by switching to another zigzag **P** conformation. This would be consistent with the remarkably low miscibility of (*R*)-**4** relative to (*R*)-**3** and (*R*)-**2**.

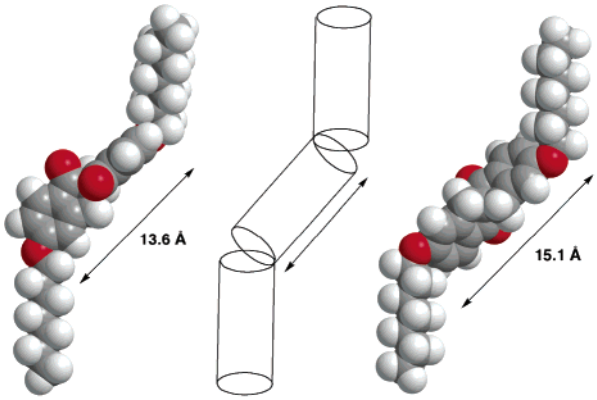

Figure 11. Space-filling models of the conformations **P** (left) and $\mathbf{C_2}$ (right) for (*R*)-**2** in relation to a simplified form of the zigzag binding site according to the Boulder model.

section of the host binding site becomes shorter. The trend in polarization power versus host structure for (*R*)-**2**, which shows δ_p increasing from +21 nC/cm^2 in the host with the longest core (**DFT**, 14.4 Å) to +749 nC/cm^2 in the host with the shortest core (**PhP1**, 9.7 Å), is consistent with this model.

The trends in polarization power versus host structure are different in the cases of (*R*)-**3** and (*R*)-**4**, which may be due to the added contribution of the CTF effect. Unfortunately, it is difficult to quantify the contribution of this effect, and how it might affect the conformational equilibrium of the chiral dopant, and the rotational distribution of its transverse dipole moment relative to the polar axis in a given liquid crystal host.[2,14,15] To rationalize the dependence of δ_p on the alkoxy group positions, the data in **NCB76** are deemed to be most reliable given the relatively high compatibility of this host with all three chiral dopants. The polarization power of (*R*)-**4** is 2.8 times greater than that of (*R*)-**2** in **NCB76**, which is consistent, to a first approximation, with the difference in dipole moments $\mu_\perp$ between the corresponding **P** conformations (−3.5 D vs +1.6 D, respectively). Notwithstanding the series of atropisomeric dopants that includes (*R*)-**1**, the δ_p value of −1037 nC/cm^2 for (*R*)-**4** in **NCB76** is the second highest reported thus far for a calamitic dopant.[39] In the case of (*R*)-**3** in **NCB76**, the smaller δ_p value of −144 nC/cm^2 is consistent with the more complex conformational distribution predicted by the conformational analysis, which includes competing **P** conformations of opposite $\mu_\perp$ (the dominant **P3** conformation has the smaller $\mu_\perp$ value of −1.6 D in this case).

(39) A polarization power of 1508 nC/cm^2 was reported for a derivative of 2-hydroxy-5,5-dialkyl-δ-valerolactone: Sakashita, K.; Ikemoto, T.; Nakaoka, Y.; Terada, F.; Sako, Y.; Kageyama, Y.; Mori, K. *Liq. Cryst.* **1993**, *13*, 71.

Conclusions

The compounds (*R*)-**2**, -**3**, and -**4** represent a new class of dopants with axially chiral cores for the induction of ferroelectric liquid crystals, with polarization powers that strongly depend on the core structure of the liquid crystal host. We have shown that relatively minor changes in the dopant structure, that is, moving the alkoxy side-chains from the 5,5′ to the 6,6′ positions of the spirobiindandione core, have profound effects on the induced spontaneous polarization (sign and magnitude), on dopant−host compatibility, and on the propensity of the dopant to exert chiral perturbations on the host environment. We have also demonstrated the usefulness of ^{2}H NMR spectroscopy to probe the local environment of dopant molecules and assess their miscibility in a liquid crystal host, as well as to detect short-range chiral perturbations exerted by a dopant on the host environment. The variations in sign and magnitude of δ_p as a function of alkoxy group positions may be rationalized on the basis of an analysis of zigzag conformations that conform to the binding site of the SmC phase according to the Boulder model. The analysis suggests that δ_p is a function of an equilibrium between two zigzag conformations with opposite dipole moments along the polar axis of the SmC* phase and that the observed host dependence may be understood in terms of differences in steric demand between the two conformations in the core region of the binding site, a new form of molecular recognition in smectic phases. A closer examination of the two opposite conformations also reveals that it may be possible to further bias the conformational equilibrium toward the **P** conformer, and therefore test our conformational distribution model, by introducing a substituent at the 6-position of one indanone fragment in (*R*)-**2**, for example. The substituent would force one alkoxy group in an *anti*-periplanar conformation relative to the carbonyl group, which is only present in the **P** conformer (Figure 9). The study of such derivatives is in progress and will be reported in due course.

Acknowledgment. We are grateful to the Natural Science and Engineering Research Council of Canada, the Canada Foundation for Innovation, and the Ontario Challenge Fund for support of this work. We also thank Profs. Ed Samulski and Elliott Burnell and Dr. Louis Madsen for useful discussions of the ^{2}H NMR results.

Supporting Information Available: Full experimental details including synthetic procedures, physical measurements and calculation methods, ^{2}H NMR spectrum of (*R*)-**4** in **5OCB**, and P_o versus x_d plots for (*R*)-**2**, -**3**, and -**4** in all four hosts. This material is available free of charge via the Internet at http://pubs.acs.org.

JA054322K